Robotica (2013) volume 31, pp. 25–33. © Cambridge University Press 2012
doi:10.1017/S0263574712000070

Alternative trajectory-tracking control approach for marine surface vessels with experimental verification

Farbod Fahimi† and Chris Van Kleeck‡

†*Department of Mechanical and Aerospace Engineering, The University of Alabama in Huntsville, Huntsville, AL 35899, USA*
‡*Department of Mechanical Engineering, University of Alberta, Edmonton, AB T6G 2G8, Canada*

(Accepted February 6, 2012. First published online: March 8, 2012)

SUMMARY
Experiments with a nonlinear trajectory-tracking controller for marine unmanned surface vessels are reported. The tracking controller is designed using a nonlinear robust model-based sliding mode approach. The marine vehicles can track arbitrary desired trajectories that are defined in Cartesian coordinate as continuous functions of time. The planar dynamic model used for the controller design consists of 3 degrees of freedom (DOFs) of surge, sway, and yaw. The vessel only has two actuators, so the vessel is underactuated. Therefore, only two outputs, which are functions of the 3-DOF, can be controlled. The Cartesian position of a control point on the vessel is defined as the output. The orientation dynamics is not directly controlled. It has been previously shown that the orientation dynamics, as the internal dynamics of this underactuated system, is stable. The result of field experiments show the effectiveness of tracking control laws in the presence of parameter uncertainty and disturbance. The experiments were performed in a large outdoor pond using a small test boat. This paper reports the first theoretical development and experimental verification of the proposed model-based nonlinear trajectory-tracking controller.

KEYWORDS: Control of robotic systems; Navigation, Unmanned surface vessels; Nonlinear control; Trajectory-tracking; Field experiments.

1. Introduction

Nowadays, the most common application of marine unmanned surface vessels is surveillance. For this application, these vehicles must be operational for extended periods of time. Currently, human operators remotely control the unmanned surface vessels. It is desirable to minimize the need for full-time, low-level human operator control, thus freeing human resources to control more vessels in a high-level supervisory mode of operation. The goal of this research is two-fold. The low-level control of single unmanned surface vessels must be automated, while the controller supports the maneuverability of the vessels on arbitrary curves with a defined time-dependent speed profile. This type of control is commonly known as trajectory tracking control.

* Corresponding author. E-mail: fahimi@eng.uah.edu

Trajectory tracking control is fundamentally different from way-point control, which is a related research topic. In way-point control, a series of desired locations (points) and the desired orientation of the surface vessel at these locations are defined. The way-point controller controls the vessel such that it meets these locations and orientations. The trajectory of the vessel while it moves from one way-point to the next is not specified, and is only generated by the controller as the controller tries to meet the next way-point. There are many publications related to way-point control; however, here the literature survey is focused on trajectory tracking control, which is the main topic of this paper.

Trajectory tracking control is especially challenging for unmanned surface vessels because of their underactuated dynamics. That is, for a surface vessel, the number of degrees of freedom (DOF) in a planar motion (3) is higher than the number of control inputs (2). In addition, for surface vessels, no kinematic constraint exists among the derivatives of DOF. The result of a literature survey on the subject, listed in Table I, shows that many researchers have introduced different methods for trajectory tracking control of surface vessels. The backstepping method, cascade control, fuzzy control, linear-quadratic-Gaussian (LQG) feedback, sliding mode, state feedback, and neural networks, with a mix of linear and nonlinear methods, have been used.

Despite using different control methods and dynamic models, in all the cited references, either of the following outputs are considered for the controller:

- Only the two-dimensional (2D) position of the center of gravity (CG) of the vessel is considered as the output of the controller, and the orientation of the vessel is not fed back. This approach may work in theory, and in practice under low disturbance levels. This is because the orientation of the vessel is inherently stable due to longitudinal hydrodynamic forces while the vessel moves. However, in practice under high disturbances, the disturbances from the water current, wave, etc. disturb the orientation of the vessel, which eventually affects the trajectory of the vessel. Since the controller only feeds back the position of CG, it cannot directly react to change in orientation. In extreme cases, the vessel may end up going backwards (180° shift in orientation) while its CG is following the desired trajectory.

https://doi.org/10.1017/S0263574712000070 Published online by Cambridge University Press

Table I. Review of unmanned surface vessel control.

Ref.	Approach	Method	Control point	Experiment	Year
[1]	Linear	LQG feedback	CG	Outdoor	1996
[2]	Linear	LQG feedback	CG	Outdoor	1997
[3]	Linear	LQG feedback	CG	No	1998
	Linear	Cascade control	CG	No	1998
[4]	Nonlinear	Backstepping	CG	No	1998
[5]	Linear	Backstepping	CG	No	1999
[6]	Nonlinear	Backstepping	CG	Indoor	2001
[7]	Nonlinear	Backstepping	CG	No	2003
[8]	Nonlinear	Fuzzy control	CG	No	2003
[9]	Nonlinear	Backstepping	CG	No	2003
[10]	Linear	Cascade control	CG	Indoor	2003
[11]	Nonlinear	Cascade control	CG	Indoor	2004
[12]	Nonlinear	PI-type sliding mode	CG	No	2004
[13]	Nonlinear	State feedback	CG	No	2005
[14]	Nonlinear	Backstepping	CG	No	2005
[15]	Nonlinear	Neural network	CG	No	2005
[16]	Nonlinear	Backstepping	CG	No	2006
[17]	Nonlinear	Fuzzy control	CG	No	2007
[18]	Nonlinear	Sliding mode	CG	No	2007
[19]	Nonlinear	Sliding mode	CG	Indoor	2008
[20]	Nonlinear	PID vs. fuzzy	CG	No	2009

- Both the 2D position of the CG and the orientation of the vessel are considered as the outputs of the controller. When this approach is used for underactuated vessels, it is attempted to control three DOFs of the vessel with only two inputs. In that case, the convergence of the vessel's DOFs to only a vicinity of the desired trajectory can be guaranteed. So there will always be a compromise between the accuracy of tracking of 3 DOFs, which causes poor performance.[21]

Another approach that improves the performance of trajectory tracking controllers is presented in this paper. Here the concept of shifting the control point is first tried for trajectory tracking of underactuated surface vessels. A control point is an arbitrary point on the vessel other than its CG, whose position is controlled for tracking a trajectory. The use of this concept has been reported for nonholonomic mobile robots in the robotics literature. However, since the kinematics, dynamics, and work environment of underactuated surface vessels are not comparable to that of mobile robots by any stretch of imagination, until now there has not been any proof that this concept would work for underactuated surface vessels. In this research, for the first time, the idea of using a control point for trajectory tracking control of surface vessels is theoretically and experimentally investigated.

The position of the control point is a function of all 3 DOFs of the vessel, the two position components of the center of mass, and the orientation of the vessel. When the position of the control point is defined as the output of the controller, any disturbance in any of the vessel's DOFs generates an output error. So the controller reacts to disturbance of the orientation as well, leading to a faster correction of the trajectory.

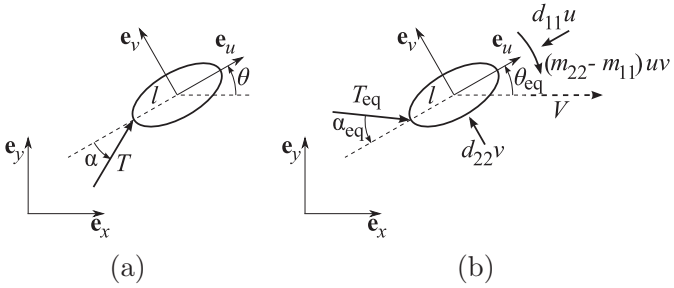


Fig. 1. Schematic diagram of the surface vessel: (a) general configuration, (b) force balance at undesirable stable equilibrium orientation while moving on a straight line with a constant speed.

2. Zero-Dynamics Stability and Control Point

Whenever an underactuated system is controlled, it has to be proved that the uncontrolled DOFs in the closed-loop system have inherent stable responses and a desirable equilibrium point. If the uncontrolled DOFs in the closed-loop system are unstable, they will cause the whole system to become unstable. And if the uncontrolled DOFs have undesirable equilibrium points, the closed-loop system may not be practical to use. None of the references cited in Table I that consider underactuated surface vessels have *directly* addressed this problem.

An example is considered to illustrate the problem arising from neglecting the zero-dynamics of an underactuated surface vessel when the CG position components are used as control outputs and the orientation is not fed back. An underactuated surface vessel is considered. The vessel is actuated by propellers and rudders. The resultant force of the propellers and rudders is presented by a single force T with an angle α with the longitudinal axis of the vessel (Fig. 1(a)). The equations of motion of the vessel, expressed in local frame ($\mathbf{e}_u$, $\mathbf{e}_v$), are

$$\begin{aligned} m_{11}\dot{u} - m_{22}vr + d_{11}u &= T\cos\alpha, \\ m_{22}\dot{v} + m_{11}ur + d_{22}v &= T\sin\alpha, \\ m_{33}\dot{r} + (m_{22} - m_{11})uv + d_{33}r &= -(T\sin\alpha)l, \end{aligned} \tag{1}$$

where u, v, and r are the surge, sway, and yaw speeds, respectively. Note that if the CG position components are used as control outputs and the orientation is not fed back for this vessel, the uncontrolled DOF, i.e. the orientation of the vessel, has an undesirable equilibrium point. As an example, it is assumed that the closed-loop controller makes the CG track a simple straight line trajectory with constant speed $V > 0$. For this trajectory, $\dot{u}$, $\dot{v}$, $\dot{r}$, r are zero, and $u = V\cos\theta_{eq}$, $v = -V\sin\theta_{eq}$, where θ_{eq} is the orientation of the vessel with respect to the desired straight line path (Fig. 1(b)). For this case, Eqs. (1) take the following form:

$$d_{11}V\cos\theta_{eq} = T_{eq}\cos\alpha_{eq}, \tag{2}$$

$$-d_{22}V\sin\theta_{eq} = T_{eq}\sin\alpha_{eq}, \tag{3}$$

$$(m_{22} - m_{11})V^2\sin\theta_{eq}\cos\theta_{eq} = -(T_{eq}\sin\alpha_{eq})l. \tag{4}$$

The state of equilibrium for this scenario is shown in Fig. 1(b). The two trivial solutions for these simultaneous

https://doi.org/10.1017/S0263574712000070 Published online by Cambridge University Press

zero-dynamic equilibrium equations are

$$\theta_{eq} = 0 \quad \alpha_{eq} = 0 \quad T_{eq} = d_{11}V, \tag{5}$$

and

$$\theta_{eq} = \pi \quad \alpha_{eq} = 0 \quad T_{eq} = -d_{11}V. \tag{6}$$

A nontrivial solution for θ_{eq} is found by solving Eqs. (2) and (3) for $\cos\theta_{eq}$ and $\sin\theta_{eq}$, respectively, and substituting the results in Eq. (4). Then the resulting Eq. (4) is solved for $T_{eq}\cos\theta_{eq}$, which is then substituted in Eq. (2). The result is

$$\theta_{eq} = \pm \arccos\left[\frac{ld_{22}}{V(m_{22} - m_{11})}\right]. \tag{7}$$

Also,

$$\alpha_{eq} = -\arctan\left[\frac{d_{22}}{d_{11}}\tan\theta_{eq}\right], \tag{8}$$

$$T_{eq} = \frac{d_{11}V\cos\theta_{eq}}{\cos\alpha_{eq}}. \tag{9}$$

It is shown that under some circumstances this equilibrium point is a stable one. The dynamics of the orientation around the equilibrium point is considered, for which $\theta = \theta_{eq} + \delta$. Note that $\dot{\theta} = \dot{\delta}$ and $\ddot{\theta} = \ddot{\delta}$. Also,

$$\sin\theta \approx \sin\theta_{eq} + \delta\cos\theta_{eq}, \tag{10}$$

$$\cos\theta \approx \cos\theta_{eq} - \delta\sin\theta_{eq}. \tag{11}$$

These relations are substituted in Eq. (1), and it is assumed that δ^2 is negligible,

$$m_{33}\ddot{\delta} + d_{33}\dot{\delta} + (m_{22} - m_{11})V^2(\cos^2\theta_{eq} - \sin^2\theta_{eq})\delta = C, \tag{12}$$

where $C = -(T_{eq}\sin\alpha_{eq})l - (m_{22} - m_{11})V^2\sin\theta_{eq}\cos\theta_{eq} = 0$ (see Eq. (4)). Note that m_{33}, d_{33}, and $m_{22} - m_{11}$ are positive. If $\cos^2\theta_{eq} - \sin^2\theta_{eq}$ is greater than zero, the the second-order differential Eq. (12) has a stable equilibrium point of $\delta_{eq} = 0$. A θ_{eq} is considered that is either in the first or the fourth quadrant. It can be concluded that

$$\cos^2\theta_{eq} - \sin^2\theta_{eq} > 0 \Rightarrow \tan^2\theta_{eq} > 1 \Rightarrow -\frac{\pi}{4} < \theta_{eq} < \frac{\pi}{4}, \tag{13}$$

or

$$\frac{\sqrt{2}}{2} < \cos\theta_{eq} < 1, \tag{14}$$

which is then combined with Eq. (7). The result is

$$\frac{\sqrt{2}}{2} < \frac{ld_{22}}{V(m_{22} - m_{11})} < 1,$$

$$\frac{\sqrt{2}}{2}\frac{m_{22} - m_{11}}{ld_{22}} < \frac{1}{V} < \frac{m_{22} - m_{11}}{ld_{22}}. \tag{15}$$

Condition (15) results in

$$\frac{ld_{22}}{m_{22} - m_{11}} < V < \sqrt{2}\frac{ld_{22}}{m_{22} - m_{11}}. \tag{16}$$

So, it can be concluded that if V satisfies condition (16), the nontrivial equilibrium point θ_{eq} exists and is stable. So if disturbances are high enough, they can bring the vessel's orientation close to this equilibrium point, and it is likely that the vessel retains this orientation while moving with the desired constant speed V on the desired straight line trajectory!

The above problem can be solved by trying to control all 3 DOFs. However, this type of control for an underactuated system can only lead to a trade-off between the tracking accuracy of each DOF. If accurate tracking of a position trajectory is desirable, a better approach must be taken.

The undesirable equilibrium point for orientation can be eliminated while the position tracking accuracy can be improved if the position components of a point attached to the vessel other than its CG are used as control outputs. Such a point is called a "control point." For a convenient formulation, the control point is assumed to be on the longitudinal axis of the vessel.

The details of the zero-dynamic stability analysis for the vessel used for experiments in this paper is found in ref. [22], where relative distances of two adjacent vessels with respect to each other are controlled (i.e. formation control). It was shown that when the control point is used for a straight line desired motion, the only stable equilibrium point is $\theta_{eq} = 0$. It was also shown that for a circular desired motion with a desired constant speed, the offset between the longitudinal axis of the vessel and the velocity vector of its CG is a known stable constant. In addition, it was discussed how the distance of the control point to the CG affects the zero-dynamic response of the orientation DOF. Since the location of the control point is a design decision, it can be chosen to lead to a desirable zero-dynamic response quality for the range of operational conditions for the vessel.

So far, it is established that the use of position components of the control point for trajectory tracking eliminates undesirable equilibrium points for the uncontrolled orientation DOF. Although the orientation of the vessel is not directly controlled in the proposed approach, it is shown in ref. [22] that the orientation is in fact inherently stable with a desirable damped dynamics and an acceptable stable equilibrium point and does not need to be controlled. Now, a robust controller must be designed to accurately control the position of the control point.

https://doi.org/10.1017/S0263574712000070 Published online by Cambridge University Press

3. Controller Design

3.1. Dynamic model

A dynamic model of a surface vessel with the state vector $\mathbf{q} = [x_c, y_c, \theta]^T$ is considered, where x_c and y_c indicate the global position components of the vessel's CG, and θ is the vessel's orientation. The velocity components of the vessel's CG in its local frame ($\mathbf{e}_u, \mathbf{e}_v$) and yaw rate ($r = \dot{\theta}$) are arranged as $\mathbf{v} = [u, v, r]^T$. It is assumed that the two physical control inputs for this vessel are a propeller speed (n) and a rudder angle (α). The dynamic equation of motion in local frame of the vessel[23] and the kinematic equation relating velocity components in the global frame to those in the local frame are

$$\mathbf{M}\dot{\mathbf{v}} + \mathbf{C}(\mathbf{v})\mathbf{v} + \mathbf{D}\mathbf{v} = \mathbf{F}, \tag{17}$$

$$\dot{\mathbf{q}} = \mathbf{R}(\theta)\mathbf{v}, \tag{18}$$

where $\mathbf{M}$ and $\mathbf{D}$ are the diagonal added-mass and damping matrices, respectively. The matrix $\mathbf{C}(\mathbf{v})$ consists of inertial forces due to Coriolis acceleration,

$$\mathbf{C}(\mathbf{v}) = \begin{bmatrix} 0 & 0 & -m_{22}v \\ 0 & 0 & m_{11}u \\ m_{22}v & -m_{11}u & 0 \end{bmatrix}. \tag{19}$$

The vector $\mathbf{F} = [T\cos\alpha, T\sin\alpha, -lT\sin\alpha]^T$ contains the longitudinal and lateral components of the propeller force (T), and the propeller's moment about the vessel's CG, which has a longitudinal offset l with the propeller location on the vessel. The matrix $\mathbf{R}(\theta)$ transforms the vessel's local frame to the global frame.

$$\mathbf{R}(\theta) = \begin{bmatrix} \cos\theta & -\sin\theta & 0 \\ \sin\theta & \cos\theta & 0 \\ 0 & 0 & 1 \end{bmatrix}. \tag{20}$$

The propeller force is modeled as $T = A|n|n$, where A is a constant, and n is the propeller speed. The local propeller force can be written as $\mathbf{F} = [AU_1, AU_2, -AlU_2]^T$, where

$$U_1 = |n|n\cos\alpha, \quad U_2 = |n|n\sin\alpha \tag{21}$$

are selected as mathematical control inputs. Now, $\mathbf{F}$ can be built by a matrix multiplication,

$$\mathbf{F} = \begin{bmatrix} A & 0 \\ 0 & A \\ 0 & -Al \end{bmatrix} \begin{bmatrix} U_1 \\ U_2 \end{bmatrix} = \mathbf{A}\mathbf{u}. \tag{22}$$

Differentiating Eq. (18) with respect to time and using Eq. (17) to substitute for $\dot{\mathbf{v}}$ and rearranging lead to the following second-order dynamic equation:

$$\begin{aligned} \ddot{\mathbf{q}} &= [\mathbf{R}(\theta)\mathbf{M}^{-1}\mathbf{A}]\mathbf{u} + [(\dot{\mathbf{R}}(\theta) - \mathbf{R}(\theta)\mathbf{M}^{-1}(\mathbf{C}(\mathbf{v}) + \mathbf{D}))\mathbf{v}] \\ &= \mathbf{b}_c\mathbf{u} + \mathbf{f}_c. \end{aligned} \tag{23}$$

3.2. Input–output equation

A control point is defined on a longitudinal axis of the vessel at a distance d with the vessel's CG toward the front of the vessel. The global position of a control point is selected as the controller output. The distance of the control point with the CG (d) affects the stability of the vessel's orientation, which is not directly controlled. The effect of this distance on directional stability is discussed in ref. [22] in detail.

The position of the control point $\mathbf{z} = [x_p, y_p]^T$ can be written as

$$\mathbf{z} = \mathbf{q}_c + d\,\mathbf{e}_u(\theta), \tag{24}$$

where $\mathbf{q}_c = [x_c, y_c]^T$ is the CG's global position, and $\mathbf{e}_u(\theta) = [\cos\theta, \sin\theta]^T$ is the unit vector describing the longitudinal axis of the vessel. The vector $\mathbf{q}_c$ is written in terms of the vector $\mathbf{q}$ as

$$\mathbf{q}_c = \begin{bmatrix} 1 & 0 & 0 \\ 0 & 1 & 0 \end{bmatrix} \mathbf{q} = \mathbf{T}\mathbf{q}. \tag{25}$$

Substituting Eq. (25) in Eq. (24), differentiating the result twice with respect to time, and substituting for $\ddot{\mathbf{q}}$ from Eq. (23) in the resulting expression, lead to the following input–output equation:

$$\begin{aligned} \ddot{\mathbf{z}} &= [\mathbf{T}\mathbf{b}_c]\mathbf{u} + [\mathbf{T}\mathbf{f}_c + d\ddot{\mathbf{e}}_u(\theta)] \\ &= \mathbf{b}\mathbf{u} + \mathbf{f}, \end{aligned} \tag{26}$$

where

$$\ddot{\mathbf{e}}_u(\theta) = [-(\ddot{\theta}\sin\theta + \dot{\theta}^2\cos\theta) \quad \ddot{\theta}\cos\theta - \dot{\theta}^2\sin\theta], \tag{27}$$

and

$$\mathbf{b} = \begin{bmatrix} \dfrac{\cos\theta A}{m_{11}} & \dfrac{\sin\theta A}{m_{22}} \\ -\dfrac{\sin\theta A}{m_{11}} & \dfrac{\cos\theta A}{m_{22}} \end{bmatrix}. \tag{28}$$

It can be seen that the determinant of $\mathbf{b} = \frac{A^2}{m_{11}m_{22}} \neq 0$, so $\mathbf{b}$ is always invertible.

3.3. Sliding model controller

The input–output system (26) is considered with the nominal system parameters, which are not necessarily accurate,

$$\ddot{\mathbf{z}} = \hat{\mathbf{b}}\mathbf{u} + \hat{\mathbf{f}}. \tag{29}$$

In the above equation, the notation "hat" indicates that the corresponding matrices are calculated using the nominal parameters of the dynamic system. The exact actual parameters of the dynamic system are always unknown. However, it is assumed that the bound of inaccuracy (uncertainty) of parameters can be determined, for example, by a sensitivity analysis of any identification method that has been used for estimating dynamic parameters. New uncertainty matrices are defined based on the bounds of the

https://doi.org/10.1017/S0263574712000070 Published online by Cambridge University Press

uncertain dynamic parameters,

$$\boldsymbol{\gamma} = \mathbf{f} - \hat{\mathbf{f}}, \tag{30}$$

$$\boldsymbol{\delta} = \mathbf{b}\hat{\mathbf{b}}^{-1} - \mathbf{I}_e. \tag{31}$$

The matrix $\mathbf{I}_{e(2\times2)}$ is an identity matrix. Here, $\mathbf{b}$ and $\mathbf{f}$ are calculated using the limits of the uncertain dynamic parameters. Note that if no uncertainty is present in the parameters of the dynamic model, both the uncertainty matrices $\boldsymbol{\gamma}$ and $\boldsymbol{\delta}$ are zero. Upper bounds are defined for the uncertainty in the components of these matrices,

$$\Gamma_i \geq |\gamma_i| \qquad i = 1, 2, \tag{32}$$

$$\Delta_{ij} \geq |\delta_{ij}| \qquad i, j = 1, 2. \tag{33}$$

Notations γ_i and δ_{ij} represent the components of matrices $\boldsymbol{\gamma}$ and $\boldsymbol{\delta}$, respectively. These components are rearranged in matrices $\boldsymbol{\Gamma}_{(2\times1)}$ and $\boldsymbol{\Delta}_{2\times2}$, respectively. The desired trajectory of the control point is defined as $\mathbf{z}^d$. Then the instantaneous error in the outputs are calculated,

$$\tilde{\mathbf{z}} = \mathbf{z} - \mathbf{z}^d. \tag{34}$$

A first-order error behavior is defined,

$$\mathbf{s} = \dot{\tilde{\mathbf{z}}} + \boldsymbol{\Lambda}\tilde{\mathbf{z}}. \tag{35}$$

In Eq. (35), $\boldsymbol{\Lambda}_{(2\times2)}$ is a positive definite matrix. Each element of the column vector $\mathbf{s} = [s_1, s_2]^T$ represents a "surface" in the phase plane corresponding to each output. A controller must be designed to ensure that (a) $\mathbf{s}$ asymptotically approaches zero despite model parameter uncertainties, and (b) the trajectory of error in the phase plane "slides" along the surface to the dynamic equilibrium point. The portion of the control law that controls the error trajectory along the sliding surface ($\mathbf{s} = \mathbf{0}$) is called equivalent control. The equivalent control is calculated by substituting the surface Eq. (35) with $\mathbf{s} = \mathbf{0}$ in the nominal input–output model (29). This results in

$$\mathbf{u}_{\text{eq}} = \hat{\mathbf{b}}^{-1}(-\hat{\mathbf{f}} + \dot{\mathbf{s}}_r), \tag{36}$$

where

$$\mathbf{s}_r = \dot{\mathbf{z}}^d - \boldsymbol{\Lambda}\tilde{\mathbf{z}}. \tag{37}$$

The equivalent control (36) is completed by adding another term to ensure that $\mathbf{s}$ asymptotically approaches zero despite model parameter uncertainties,

$$\mathbf{u} = \mathbf{u}_{\text{eq}} - \hat{\mathbf{b}}^{-1}\begin{bmatrix}\text{sgn}(s_1) & 0\\ 0 & \text{sgn}(s_2)\end{bmatrix}\mathbf{K} \tag{38}$$

$$= \mathbf{u}_{\text{eq}} - \hat{\mathbf{b}}^{-1}\,\text{sgn}(\mathbf{s})\mathbf{K}. \tag{39}$$

The matrix $\mathbf{K}_{(2\times1)}$ is a column gain matrix, whose elements must be determined to guarantee the asymptotic stability of $\mathbf{s}$. A Lyapunov function is defined as

$$V = \frac{1}{2}\mathbf{s}^T\mathbf{s}. \tag{40}$$

The rate of change of this Lyapunov function is calculated,

$$\dot{V} = \mathbf{s}^T\dot{\mathbf{s}} = \mathbf{s}^T(\ddot{\mathbf{z}} - \dot{\mathbf{s}}_r). \tag{41}$$

The actual (as opposed to nominal) $\ddot{\mathbf{z}}$ is determined using Eq. (26) with the control law (39),

$$\dot{V} = \mathbf{s}^T(\mathbf{f} + \mathbf{b}\mathbf{u} - \dot{\mathbf{s}}_r) \tag{42}$$

$$= \mathbf{s}^T(\mathbf{f} + \mathbf{b}\hat{\mathbf{b}}^{-1}(-\hat{\mathbf{f}} + \dot{\mathbf{s}}_r - \text{sgn}(\mathbf{s})\mathbf{K}) - \dot{\mathbf{s}}_r). \tag{43}$$

Substituting Eq. (31) into Eq. (43) and rearranging results in the following form,

$$\dot{V} = \mathbf{s}^T(\mathbf{f} - \hat{\mathbf{f}} + \boldsymbol{\delta}(-\hat{\mathbf{f}} + \dot{\mathbf{s}}_r) + (-\boldsymbol{\delta} - \mathbf{I}_e)\text{sgn}(\mathbf{s})\mathbf{K}). \tag{44}$$

To incorporate the bounds of uncertainty in the parameters of the dynamic model, the above equation is manipulated,

$$\dot{V} \leq \mathbf{s}^T(\boldsymbol{\Gamma} + \boldsymbol{\Delta}| - \hat{\mathbf{f}} + \dot{\mathbf{s}}_r| + (\boldsymbol{\Delta} - \mathbf{I}_e)\text{sgn}(\mathbf{s})\mathbf{K}). \tag{45}$$

Expanding Eq. (45), factoring $|s_1|$ and $|s_2|$ and rearranging them in a vector $\text{abs}(\mathbf{s}^T) = [|s_1|, |s_2|]$ result in the following form,

$$\begin{aligned}\dot{V} &\leq -\text{abs}(\mathbf{s}^T)(-\boldsymbol{\Gamma} - \boldsymbol{\Delta}| - \hat{\mathbf{f}} + \dot{\mathbf{s}}_r| - [(\boldsymbol{\Delta}_{\text{d}} - \mathbf{I}_e)\\ &\quad +\text{sgn}(s_1.s_2)\boldsymbol{\Delta}_{\text{od}}]\mathbf{K})\\ &\leq -\text{abs}(\mathbf{s}^T)\boldsymbol{\eta}.\end{aligned} \tag{46}$$

In Eq. (46), matrices $\boldsymbol{\Delta}_{\text{d}}$ and $\boldsymbol{\Delta}_{\text{od}}$ comprise the diagonal and off-diagonal elements of matrix $\boldsymbol{\Delta}$, respectively. Note that the rate of the Lyapunov function V is always negative if the column vector $\boldsymbol{\eta}_{(2\times1)}$ has positive elements at all times. In other words, if the column gain matrix $\mathbf{K}$ is calculated from the following equation,

$$\mathbf{K} = [(\mathbf{I}_e - \boldsymbol{\Delta}_{\text{d}}) - \text{sgn}(s_1.s_2)\boldsymbol{\Delta}_{\text{od}}]^{-1}(\boldsymbol{\Gamma} + \boldsymbol{\Delta}| - \hat{\mathbf{f}} + \dot{\mathbf{s}}_r| + \boldsymbol{\eta}), \tag{47}$$

where $\boldsymbol{\eta}$ has positive elements, the rate of Lyapunov function V is always negative, and, consequently, $\mathbf{s}$ asymptotically approaches zero despite bounded model parameter uncertainties. When $\mathbf{s}$ becomes zero, since $\boldsymbol{\Lambda}$ is positive definite, the tracking error $\tilde{\mathbf{z}}$ will asymptotically approach zero (see Eq. 35). This proves the asymptotic stability of the controller.

Note that the matrix $[(\mathbf{I}_e - \boldsymbol{\Delta}_{\text{d}}) - \text{sgn}(s_1.s_2)\boldsymbol{\Delta}_{\text{od}}]$ in Eq. (46) is very close to an identity matrix because uncertainty terms $\boldsymbol{\Delta}_{\text{d}}$ and $\boldsymbol{\Delta}_{\text{od}}$ are normally small. So, this matrix is most likely invertible. In the extreme case, since uncertain terms are assumed by the designer, the designer can pick values for these terms that make this matrix invertible. The control law calculates $\mathbf{u} = [U_1, U_2]^T$ in real-time. Then, based on U_1 and U_2, the physical inputs n and α are calculated

https://doi.org/10.1017/S0263574712000070 Published online by Cambridge University Press

Table II. Summary of the test vessel parameters.

Inertia:	$m_{11} = 7.8$ kg	$m_{22} = 8.4$ kg	$m_{33} = 0.4$kg m^2
Damping:	$d_{11} = 20.7$ kg/s	$d_{22} = 26.5$ kg/s	$d_{33} = 2.2$ kg m^2/s
Propellers:	$K_t = 0.13$	$D = 0.047$ m	$l = 0.21$ m
Thrust:	$\rho = 998$ kg/m^3	$A = 2K_t\rho D^4$	$A = 1.27 \times 10^{-3}$ kg m



Fig. 2. The experimental platform.

using Eqs. (21) and applied to the surface vessel. The sliding mode control method can theoretically guarantee perfect system performance in presence of nominal parameter uncertainty and disturbance whose bounds are known. Here, analyzing the sensitivity of the found dynamic parameters via the identification algorithm suggested 15% uncertainty.[22] So the controller was designed for uncertainties in the dynamic parameters of up to 20%.

4. Experimental Platform

A robotic small boat (with 7.8-kg mass and 0.8-m length) was designed and built for control experimentation purposes (Fig. 2). The base platform is that of a standard remote control small race boat. An embedded computer of PC-104 form factor with a 1.8 GHz Pentium M processor and a navigational sensor unit that outputs the vessel's state vector via an Ethernet port are the heart of the control hardware. The navigational sensor consists of a GPS unit, 3-axis accelerometers and gyroscopes, and fuses all raw data from the sensors to estimate the 6-DOF states of the vessel, including (x, y, z) position components and roll, pitch, and yaw Euler angles. The sliding mode control algorithm is coded using Matlab/Simulink and the xPC-Target rapid control prototyping software. The software runs in real-time on the embedded computer.

The parameters in the dynamic model of the vessel (Table II) are identified by performing open loop control experiments, and using optimizations. The details of the open loop experiments and identification method can be found in ref. [22].

5. Closed-Loop Control Outdoor Experiment

Several successful tests have been performed in a large outdoor pond in William Hawrelak Park, Edmonton, Alberta, Canada (N +53° 31' 38.6", W −113° 33' 2.7"). The result of two tests performed on different days are reported in this paper. Test (a), whose tracking errors are among the largest in all our tests, was done on a day when the local weather station reported wind gust speeds of 10 to 15 km/h. Test (b), whose tracking errors are among the smallest in all our tests, was done on a calm day.

For the closed-loop experiments, a smooth 8-shaped desired trajectory is defined. This trajectory consists of two circular arcs that are connected by two seven-order polynomials. The coefficients of the polynomial terms were calculated such that the trajectory is continuous at the junctions of the arcs and the polynomials up to jerk (time derivative of acceleration). The desired speed for the vessel as it enters the desired trajectory is 0.25 m/s. This desired speed is smoothly raised to 0.5 m/s during the first 15 s of travel on the desired trajectory.

It is important to note that discontinuous desired trajectories, e.g with 90° sharp turns, were found not to be practical to use with the sliding mode control. These kinds of trajectories easily cause input saturation at discontinuous points. The input saturation leads to practical stability problems at the discontinuous points. This is the main reason why a desired trajectory is defined that is continuous up to jerk (time derivative of acceleration).

At first, the control algorithm only consisted of the sliding mode control. However, it was found that if the outputs of the boat at the initialization of the sliding mode control were too different from the desired trajectory at time zero, the actuators would saturate and would not retrieve from saturation for some time. The actuator saturation caused practical stability problems. To solve this problem, a Proportional-Derivative (PD) way-point controller was used to initialize the control. The PD controller brought the outputs of the system close to the desired trajectory before sliding mode control was engaged. This way, the initial errors sensed by the sliding mode control at initialization were small, and input saturation was prevented.

So the final tested control algorithm consists of two parts. The first part is a simple PD way-point controller, and the second part is the robust sliding mode trajectory-tracking controller. The PD controller is responsible for driving the vessel to the start point of the desired trajectory on a straight line with a pre-defined speed of 0.25 m/s. When the controller detects that the vessel is at a reasonably small distance from the start point of the desired trajectory, it switches from the PD way-point control to the robust sliding mode trajectory-tracking control.

The control program is initiated and run when the vessel is at shore. This moment is the origin of time, at which recording of the time and the vessel states begin at 100 Hz. The default mode of the control program is manual control.

https://doi.org/10.1017/S0263574712000070 Published online by Cambridge University Press

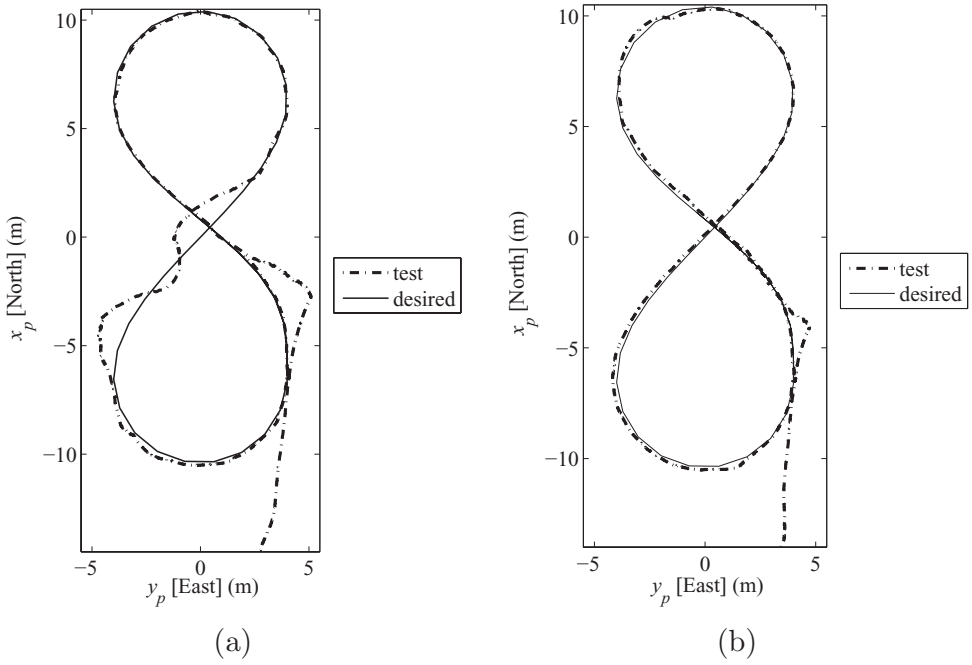


Fig. 3. The path of the control point of the vessel recorded in real-time: (a) A windy day (10–15 km/h gusts); (b) a calm day.

An operator drives the vessel via remote control to a point to the south of the desired trajectory start point. When the operator is satisfied with the initial location of the vessel, he triggers the automatic controller (at 143.24 s and 122.59 s for the reported tests (a) and (b), respectively), which runs at 100 Hz. Driven by the PD way-point control, the vessel arrives at the start point of the desired trajectory (at 158.24 and 137.59 s for the reported tests (a) and (b), respectively), when the sliding mode control automatically takes over.

The desired trajectory and the recorded path of the vessel in real-time for the two tests are shown in Fig. 3. The vessel travels on a straight line from the point where the automatic control is engaged to the start point of the desired trajectory. At this point, the sliding mode control takes over. For some reason (explained below), in both tests (a) and (b), the vessel initially diverges from the desired trajectory when the control switch is made. The divergence is larger for test (a), where a steady wind is blowing out of West. However, in both the tests, the vessel converges to the desired trajectory in less than 10 s. The vessel follows the desired trajectory very closely for most of the duration of its motion. In test (a), the controller rejects two disturbances caused by two successive wind gusts when the vessel is on the West side of the southern arc (from 220 to 250 s). Figure 4 shows the tracking error for the two reported tests. Everywhere, except at the beginning of the trajectory and when gusts exist, the trajectory-tracking error is less than 0.25 m, which is the resolution of the on-board navigational sensor. It can be seen that between 220th and 250th s of test (a), the lateral error e_y is more sensitive to disturbances than the longitudinal error e_x. This could be related to the under-actuated nature of the vessel, which lacks direct lateral control.

Figure 5 shows the velocity components of the vessel's CG in its local coordinates. The desired longitudinal speed (u) for the vessel during the way-point control is 0.25 m/s. However, in both the tests, the PD controller drives the

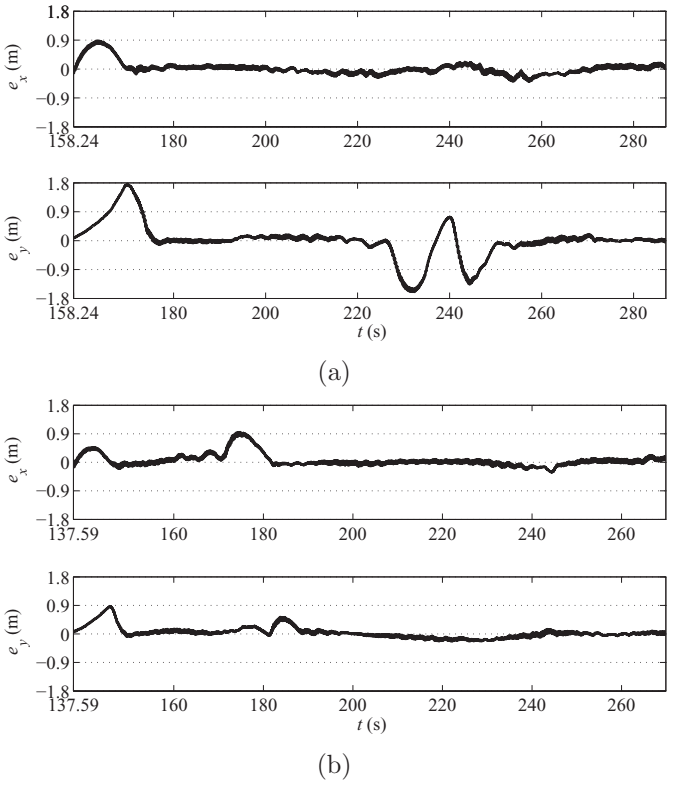


Fig. 4. Tracking error for the control point recorded in real-time: (a) A windy day (10–15 km/h gusts); (b) A calm day.

vessels at 0.5 m/s, causing a large offset in speed. The desired longitudinal speed at the beginning of the desired trajectory is also 0.25 m/s. So, when the sliding mode control takes over, it tries to slow down the vessel. Since the driveline of the vessel does not support negative propeller speeds, the controller can only shut down the propeller to zero speed. This reduces the vessel's speed as desired, but handicaps the control. That is

https://doi.org/10.1017/S0263574712000070 Published online by Cambridge University Press

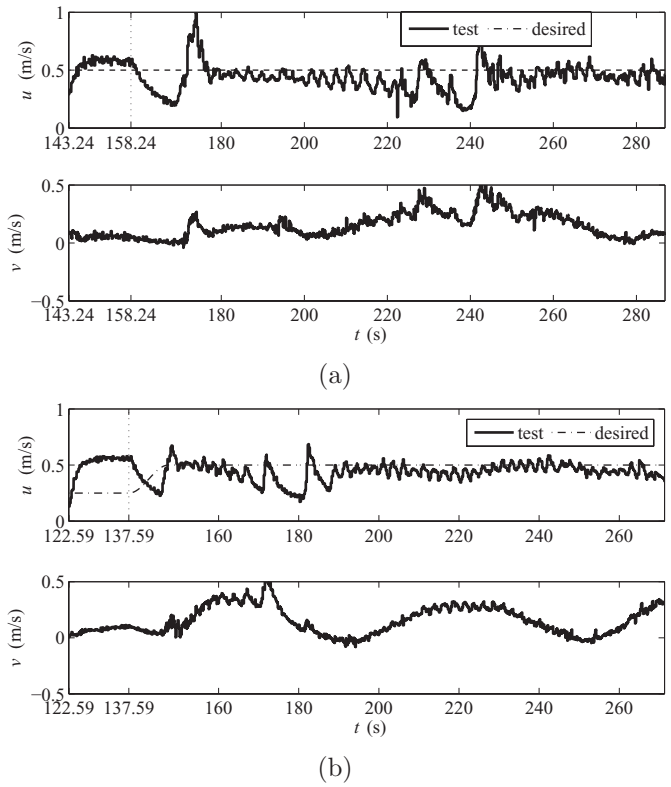


Fig. 5. Local speed components of the vessel recorded in real-time: (a) A windy day (10–15 km/h gusts); (b) a calm day.

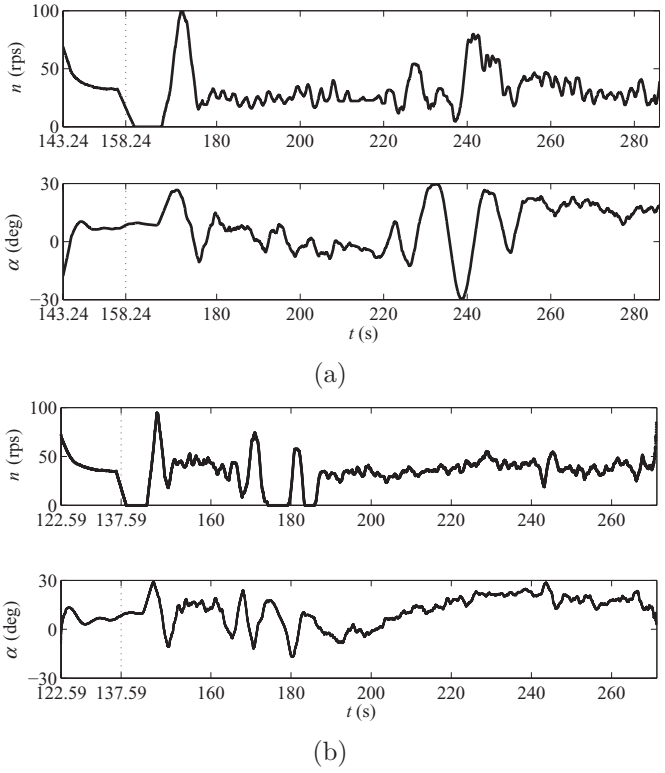


Fig. 6. Propeller speed and rudder angle recorded in real-time: (a) A windy day (10–15 km/h gusts); (b) a calm day.

why, in both the tests, the vessel initially drifts away from the desired trajectory. Since wind blows out of West during test (a), this drift is larger for that test. It is interesting to note that the lateral velocity component is non-zero at times for both the tests. This means that the vessel does not move tangent to its path when the path is curved.

The control inputs are shown in Fig. 6. During the time from 220 s to 250 s for test (a), the controller is reacting to the disturbance, so the inputs vary rapidly. For the rest of the test duration, the inputs do not vary too quickly. The propeller speed and the rudder angle remain well in their limits of 140 rps and $\pm 30^{\circ}$, respectively. The desired trajectory had been designed and tested in simulations such that inputs do not saturate. Figure 7 shows the global components of the velocity of the control point. Except at the beginning of the motion, where propeller is shut down, and during the disturbance period, the vessel tracks the desired velocity components very closely.

6. Conclusion

The results of experimentation with a robust sliding mode trajectory tracking controller for unmanned surface vessels is presented. The test vessel is a small boat that is tested in an outdoor pond. The nonlinear dynamic model of the vessel has been previously identified, and is used in this research. A sensitivity analysis of the identification result is used to determine the bounds of the uncertainty in identified parameters. The sliding mode controller is designed to overcome the uncertainties. A smooth 8-shaped desired trajectory is defined. The outdoor tests show that

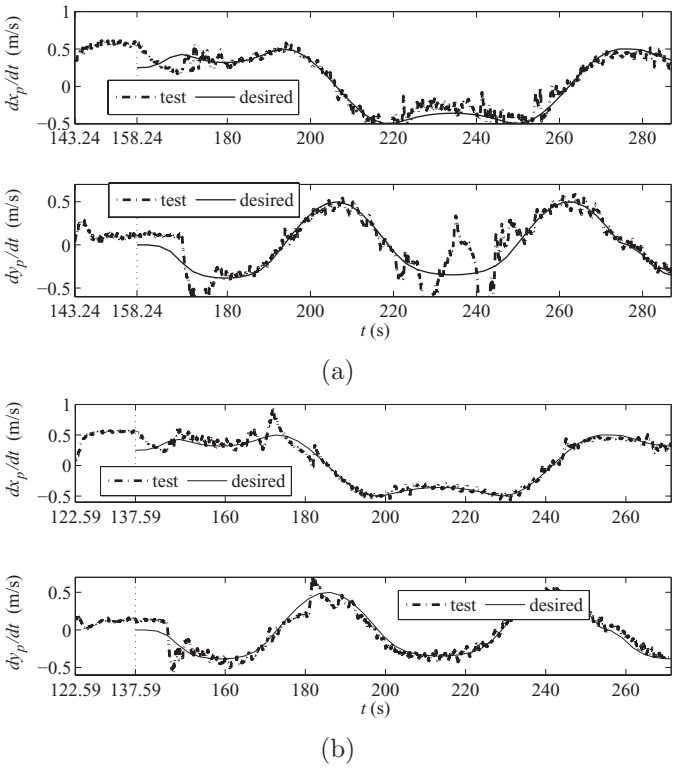


Fig. 7. Global components of the velocity of the control point recorded in real-time: (a) A windy day (10–15 km/h gusts); (b) a calm day.

https://doi.org/10.1017/S0263574712000070 Published online by Cambridge University Press

the controller can drive the boat with negligible deviation from the desired trajectory when no disturbance is present. The test also shows the ability of the controller to efficiently reject disturbances.

References

1. A. Sorensen, S. Sagatun, and T. Fossen, "Design of a dynamic positioning system using model-based control," *Control Eng. Pract.*, **4**(3), 359–368 (1996) (online). Available at: http://dx.doi.org/10.1016/0967-0661(96)00013-5
2. T. Holzhueter, "LQG approach for the high-precision track control of ships," *IEE Proc. Contr. Theor. Appl.* **144**(2), 121–127 (1997) (online). Available at: http://dx.doi.org/10.1049/ip-cta:19971032
3. L. Morawski and J. Pomirski, "Ship track-keeping: Experiments with a physical tanker model," *Control Eng. Pract.* **6**(6), 763–769 (1998) (online). Available at: http://dx.doi.org/10.1016/S0967-0661(98)00082-3
4. J.-M. Godhavn, T. Fossen and S. Berge, "Non-linear and adaptive backstepping designs for tracking control of ships," *Int. J. Adapt. Control Signal Process.* **12**(8), 649–670 (1998) (online). Available at: http://dx.doi.org/10.1002/(SICI)1099-1115(199812)12:8<649::AID-ACS515>3.0.CO;2-P
5. K. Pettersen and H. Nijmeijer, "Global practical stabilization and tracking for an underactuated ship – a combined averaging and backstepping approach," *Model. Identif. Control* **20**(4), 189–199 (1999).
6. K. Y. Pettersen and H. Nijmeijer, "Underactuated ship tracking control: Theory and experiments," *Int. J. Control* **74**(14), 1435–1446 (2001) (online). Available: http://dx.doi.org/10.1080/00207170110072039
7. M. Casado and F. Velasco, "Surface ship trajectory control using non-linear backstepping design," *Proc. Inst. Mar. Eng. Sci. Technol. A (J. Mar. Eng. Technol.* **3**, 3–8 (2003).
8. J. Velagic, Z. Vukic and E. Omerdic, "Adaptive fuzzy ship autopilot for track-keeping," *Control Eng. Practice* **11**(4), 433–443 (2003) (online). Available at: http://dx.doi.org/10.1016/S0967-0661(02)00009-6
9. K. Do, Z. Jiang and J. Pan, "Underactuated ship global tracking under relaxed conditions," *IEEE Trans. Autom. Control* **47**(9), 1529–1536 (2002) (Online). Available at: http://dx.doi.org/10.1109/TAC.2002.802755
10. E. Lefeber, K. Y. Pettersen and H. Nijmeijer, "Tracking control of an underactuated ship," *IEEE Trans. Control Syst. Technol.* **11**(1), 52–61 (Jan. 2003).
11. K. Y. Pettersen, "Global uniform asymptotic stabilization of an underactuated surface vessel: Experimental results," *IEEE Trans. Control Syst. Technol.* **12**(6), 891–903 (Nov. 2004).
12. K.-W. Yu and C.-E. Wu, "Tracking control of a ship by PI-type sliding controller," *J. Marine Sci. Technol.* **12**(3), 183–188 (2004).
13. K. Do, Z. Jiang and J. Pan, "Global partial-state feedback and output-feedback tracking controllers for underactuated ships," *Syst. Control Lett.* **54**(10), 1015–1036 (2005) (online). Available at: http://dx.doi.org/10.1016/j.sysconle.2005.02.014
14. K. D. Do and J. Pan, "Global tracking control of underactuated ships with non-zero off-diagonal terms in their system matrices," *Automatica* **41**(1), 87–95 (2005) (online). Available at: http://dx.doi.org/10.1016/j.automatica.2004.08.005
15. A. Saeed, E. Attia, A. Helmy and T. Awad, "Design of a neuro-autopilot maneuvering controller for underactuated ships," *AEJ – Alexandria Eng. J.* **44**(4), 493–500 (2005).
16. J. Ghommam, F. Mnif, A. Benali and N. Derbel, "Asymptotic backstepping stabilization of an underactuated surface vessel," *IEEE Trans. Control Syst. Technol.* **14**(6), 1150–1157 (2006) (online). Available at: http://dx.doi.org/10.1109/TCST.2006.880220
17. W. Gierusz, N. Cong Vinh and A. Rak, "Maneuvering control and trajectory tracking of very large crude carrier," *Ocean Eng.* **34**(7), 932–945 (2007) (online). Available at: http://dx.doi.org/10.1016/j.oceaneng.2006.06.003
18. J. Cheng, J. Yi and D. Zhao, "Design of a sliding mode controller for trajectory tracking problem of marine vessels," *IET Control Theory Appl.* **1**(1), 233–237 (2007) (online). Available at: http://dx.doi.org/10.1049/iet-cta:20050357
19. H. Ashrafiuon, K. R. Muske, L. C. McNinch and R. A. Soltan, "Sliding-mode tracking control of surface vessels," *IEEE Trans. Ind. Electron.* **55**(11), 4004–4012 (2008) (online). Available at: http://dx.doi.org/10.1109/TIE.2008.2005933
20. L. Gyoungwoo, S. Surendran and S.-H. Kim, "Algorithms to control the moving ship during harbour entry," *Appl. Math. Modelling* **33**(5), 2474–2490 (May 2009).
21. A. P. Aguiar and J. P. Hespanha, "Position tracking of underactuated vehicles," **In**: *Proceedings of the American Control Conference*, vol. 3, Denver, CO, USA (June 4–6, 2003), pp. 1988–1993 (online). Available at: http://dx.doi.org/10.1109/ACC.2003.1243366
22. D. Schoerling, C. Van Kleeck, F. Fahimi, C. R. Koch, A. Ams and P. Lober, "Experimental test of a robust formation controller for marine unmanned surface vessels," *Auton. Robots*. **28**(2), 213–230 (2010) (online). Available at: http://dx.doi.org/10.1007/s10514-009-9163-6
23. T. I. Fossen, *Guidance and Control of Ocean Vehicles* (John Wiley, Chichester, UK, 1994).

https://doi.org/10.1017/S0263574712000070 Published online by Cambridge University Press